URTeC: 2153641

Microseismic Event Location using Multiple Arrivals: Demonstration of Uncertainty Reduction

Zhishuai Zhang*, James W. Rector, Michael J. Nava, University of California, Berkeley.

Summary

Event location is the basis of hydraulic fracture characterization using microseismic data. However, the traditional method of using direct arrival times and P-wave polarizations leads to increased error due to the large uncertainty in polarization. Due to shale's low velocity nature and the configuration of horizontal stimulation and monitoring wells, the head wave can often be the first arrival rather than the direct arrival.

Finite difference modeling was used to validate the character of head waves in field data gathered from the Marcellus shale and the situations under which a head wave can be the first arrival were carefully analyzed. With careful processing, we reveal the presence of high number of head waves in the Marcellus Shale. Head wave and direct arrivals were used instead of the conventional P-wave polarization to estimate microseismic event location. A Bayesian inference program was also developed for joint event location and velocity model calibration. Validation of the developed method was performed on perforation shots and shows that using head waves instead of polarization can achieve much better resolution in microseismic event location. The application of the developed method on field data shows a more reasonable result than that provided by contractor.

Our results show that the head wave can be a contributor instead of a detractor in the process of accurate event location. This will eliminate the necessity for polarization which has large uncertainty due to poor geophone-borehole coupling, multiple arrivals, and low signal to noise ratio. The developed method can effectively improve the accuracy of microseismic event location and proposes a better acquisition geometry and strategy to reduce microseismic monitoring cost and improve event location accuracy.

Introduction

Hydraulic fracturing is the process of injecting fluid with high pressure that exceed the formation minimal principal stress to induce tensile fracture that can increase permeability and stimulate production of a well. Microseismic monitoring has been widely used for hydraulic fracturing monitoring and characterization since its initial implementation (Cipolla et al., 2012; Eisner et al., 2007; Maxwell, 2014; Warpinski, 2009). Microseismic acquisition geometry involves mainly surface survey (Duncan and Eisner, 2010) and downhole survey (Maxwell et al., 2010). Shallow well below water table is also an option for situations where downhole monitoring is not applicable or not adequate. For horizontal wells in shale gas production, it is a common case to have only one nearby well, the production well, available for microseismic monitoring. This kind configuration has the advantage that the geophones can be moved to the nearest place of the stimulation. Also, the deep environment eliminates the effect of noise due to surface fracturing operation and surface noise (Maxwell, 2014). However, the limit coverage of acquisition geometry makes microseismic processing difficult.

Microseismic processing involves basic location, moment magnitude estimation, and advanced source parameter and frequency analysis (Eisner et al., 2007). The event location, as the basis of almost all other advanced processing, has been routinely conducted by industry. As an inverse problem, the microseismic event location in downhole monitoring can be carried out in various ways. Commonly used methods include least-square travel time inversion (Douglas,

1967; Li et al., 2014), double-difference (Waldhauser and Ellsworth, 2000), coherence scanning (Drew et al., 2005; Duncan and Eisner, 2010), full-waveform inversion, and et al. Though effective to a certain extend, these methods don't follow a rigorous statistical framework. Thus, they may either have difficulty in predicting uncertainty with their location estimation or can only give a rough value of estimation uncertainty. Some study on the effect on locations uncertainty due to various factors has been carried out (Eisner, 2009; Maxwell, 2009). However, the source of uncertainty can be very complex in field. An engineer without in-depth of microseimic processing can be surprised by the large uncertainty within the event location (Hayles et al., 2011). It is crucial to improve microseismic events location technique before we can draw further conclusion on microseismic data.

Bayesian inversion has been widely used for subsurface inverse problem (Oliver et al., 2008; Tarantola, 2005; Tarantola and Valette, 1982; Zhang et al., 2014). Thanks to its way of treating variable as a probability density function, it has been very successful in model estimation and uncertainty analysis. The Bayesian inversion has been used for earthquake location (Myers et al., 2007; Myers et al., 2009) and microseismic event location (Poliannikov et al., 2014). However, further efford need to be put to make full use of the powerfulness of this method.

Due to the limit coverage of acquisition geometry in single horizontal monitoring well, microseismic event location with only P and S arrival times is impossible. An additional constraint on the event location usually comes from direct P-wave polarization (Dreger et al., 1998; Li et al., 2014). Thus, three component data will be necessary. However, the unknown orientation of downhole geophones and poor coupling (Gaiser et al., 1988) between geophone and borehole are the challenges to use three component data. The perforation shots were normally used for geophone orientation calibration. Because of the complexity and anisotropy of shale formation, and the poor coupling of geophones with horizontal wellbore, the uncertainty in the waveform polarization can be relatively large.

Due to shale's low velocity nature, head wave is very common in crosswell seismic (Dong and Toksöz, 1995; Parra et al., 2002; Parra et al., 2006) and microseismic survey (Maxwell, 2010; Zimmer, 2010; Zimmer, 2011) in shale operation. When the distance between geophones and source is relatively large, the head wave arrival can precede direct arrival. Microseismic industry has realized the presence of head wave before direct arrival. Due to its weakness, head wave has been commonly regarded as the contamination of direct arrival. Some preliminary research on making use of head wave has been conducted but mainly on synthetic example of simplified situations (Zimmer, 2010; Zimmer, 2011). No publication on field data and rigorous analysis on the improvement due to head wave is available. Our analysis on microseismic survey conducted on two horizontal wells in Marcellus shale shows that head wave conveys very useful information, which can eliminate the requirement for waveform polarization in microseismic event location.

In this paper, we observed and verified the existence of head wave in Marcellus shale operation. We used head wave as a substitution for direct P-wave polarization for microseismic event location estimation. To this end, a Bayesian inversion framework for velocity model calibration and uncertainty analysis was developed. The achieved result shows much better accuracy than traditional event location method.

Theory and Method

Head wave

Head wave is common in microseismic survey in shale (Maxwell, 2010; Zimmer, 2010; Zimmer, 2011). We consider a parallel horizontal wells pair configuration (Figure 1), which is common in this kind of Marcellus shale formation. When the velocity of a nearby layer (the lower layer in this case) is larger than the layer where source and receiver are situated, head wave can be present when the angle of incidence is equal to the critical angle $\arcsin(V_1/V_2)$. The head wave will then travel along the formation interface until the point where it refracted back to the original layer with angle of emergence at the critical angle. Direct arrival amplitude is inversely proportional to the distance the seismic ray traveled from the source due to geometrical spreading while head wave amplitude is inversely proportional to the square of this distance. Thus, the head wave will decay faster than direct arrival and usually has a smaller amplitude.

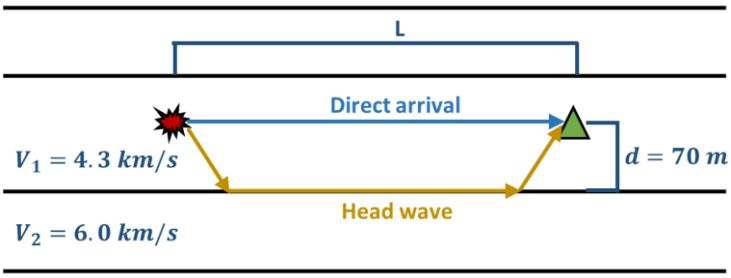

Figure 1: A common configuration for head wave in shale gas operation. Due to the low velocity nature of shale, headwave is common when there is a nearby high velocity layer. When source receiver distance is relatively large, head wave can overtake direct arrival to be the first arrival.

Though the head wave travels a longer path than the direct arrival, its speed is higher in high velocity zone. So the head wave can take over direct arrival as the first arrival when the source receiver distance is longer than the cross-over distance. For the configuration in Figure 1. The travel time of head wave, P-wave, and S-wave as a function of source receiver distance is shown by Figure 2. Here, S-wave velocity of the shale layer is taken as 4.3 km/s, and the high velocity layer is 70 meters below the geophones with 6.0 km/s S-wave as shown by Figure 1.

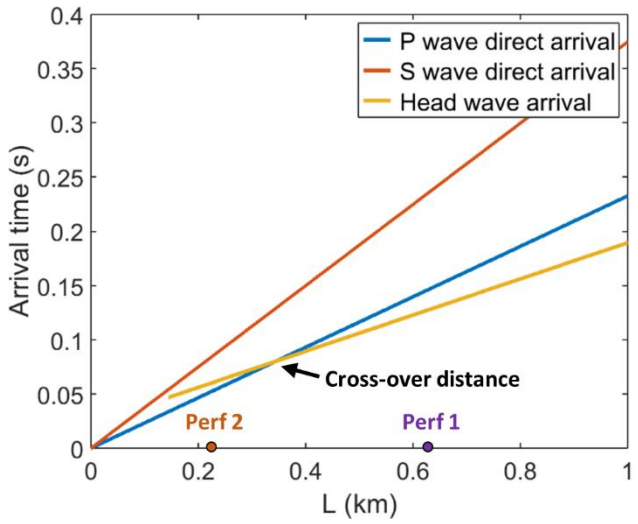

Figure 2: Arrival time of various phases as a function of source receiver distance. When source receiver distance is larger than the cross-over distance, head wave can overtake direct arrival to be the first arrival in the waveform. Perf 1 and Perf 2 are positions analyzed in later content.

Bayesian inversion for microseismic event location

To quantify probability distribution of model parameters (microseismic event locations, origin time, velocity model) and observable data (arrival time of various phases and/or direct P-wave polarization), we developed a Bayesian inference framework for microseismic event location. From inverse problem theory problem (Oliver et al., 2008; Tarantola, 2005; Tarantola and Valette, 1982; Zhang et al., 2014), we can demonstrate that under Gaussian assumption of forward model, measurement, and a priori information, we can get the a posteriori information of the model with a probability density:

$$\sigma_{\mathrm{M}}(\mathbf{m}) \propto \exp\left\{-\frac{1}{2}\left[(\mathbf{g}(\mathbf{m})-\mathbf{d}_{\mathbf{obs}})^{\mathrm{T}}\mathbf{C}_{\mathbf{D}}^{-1}(\mathbf{g}(\mathbf{m})-\mathbf{d}_{\mathbf{obs}})+(\mathbf{m}-\mathbf{m}_{\mathbf{prior}})^{\mathrm{T}}\mathbf{C}_{\mathbf{m}}^{-1}(\mathbf{m}-\mathbf{m}_{\mathbf{prior}})\right]\right\}$$

where $\mathbf{d}_{\mathbf{obs}}$ is a vector containing the observed data. In the problem of microseismic event location, it can be an array of arrival times of all pickable phases. If we choose to use polarization in addition to arrival times, the polarization should be packed into the vector as well. The data covariance matrix $\mathbf{C}_{\mathbf{D}}=\mathbf{C}_{\mathbf{d}}+\mathbf{C}_{\mathbf{T}}$ is the sum of the observation part $\mathbf{C}_{\mathbf{d}}$ and model part $\mathbf{C}_{\mathbf{T}}$. The model parameter vector $\mathbf{m}$, and its prior information $\mathbf{m}_{\mathbf{prior}}$ is the vector containing the unknown model parameters we want to estimate. In our problem, it is the space coordinate and origin time of

microseismic events. The parameters describing velocity model can also be a part of the model parameter if we want to do a joint inversion of events location and velocity model. $\mathbf{C_m}$ is the parameter covariance matrix of the prior information. The forward operator $\mathbf{g(m)}$ is a function of the model parameters $\mathbf{m}$ and will give a prediction on the observable data $\mathbf{d}$ based on the model parameters. We use a ray tracing method as the forward operator to predict the arrival time and/or polarization based on event location and origin time.

Maximum A Posteriori solution to Bayesian inversion

The solution to the posterior probability density function (PDF) of model parameter can be challenging (Oliver et al., 2008; Tarantola, 2005). Under the assumptions that the observation and the prior information on model parameters (microseismic event location and origin time) are Gaussian distribution, and the forward operator is linear, that is $\mathbf{g(m)} = \mathbf{Gm}$, the posterior probability distribution function can be Gaussian. We can solve the PDF function analytically under this Gaussian distribution. However, the linearity assumption of the forward operator $\mathbf{g(m)}$ is usually invalid, as the case of our problem.

The solutions to the non-Gaussian problem fall into two categories. The first category is representing the probability density with stochastic realizations (e.g., MCMC). And the second one is estimating the key point of the posterior PDF with deterministic approach. Here, we are going to use a Maximum A Posteriori (MAP) estimate, which fall in the second category, to characterize the posterior PDF of microseismic event location and origin time (Oliver et al., 2008; Zhang et al., 2014).

The MAP estimate method is trying to find the peak of the posterior PDF and regard the model at this point as the most likely case given the prior information and observation. This can be accomplished by minimizing the exponent of the posteriori probability density with the Gauss–Newton algorithm:

$$O(\mathbf{m}) = \frac{1}{2}(\mathbf{g(m)} - \mathbf{d_{obs}})^{\mathrm{T}}\mathbf{C_D^{-1}}(\mathbf{g(m)} - \mathbf{d_{obs}}) + \frac{1}{2}\left(\mathbf{m} - \mathbf{m_{prior}}\right)^{\mathrm{T}}\mathbf{C_m^{-1}}\left(\mathbf{m} - \mathbf{m_{prior}}\right)$$

We can also get an estimation on the posterior covariance matrix $\mathbf{C_{m,MAP}}$ with the linearization of the problem at the MAP point:

$$\mathbf{C_{m,MAP}} = \left(\mathbf{G_{MAP}^T C_D^{-1} G_{MAP}} + \mathbf{C_m^{-1}}\right)^{-1}$$

where $\mathbf{G_{MAP}}$ is the Jacobian matrix of the model parameter at the MAP point.

Microseismic Survey Overview

The hydraulic fracturing project was carried out in Marcellus formation in Susquehanna County, Pennsylvania, within Susquehanna River Basin. The primary purpose of this project is increasing stimulation efficiency by only changing operational constraints, i.e. pump rate. Two horizontal wells, Monitor well and stimulation well, were drilled at the depth of around $1500\ m$ as shown by Figure 3. The length of the horizontal portion of the two wells are 1.35 and $1.7\ km$ respectively. And the average distance between the horizontal portions of the two wells is around $0.22\ km$.

Eighteen hydraulic fracturing stages were conducted with four perforation shots per stage prior each stimulation stage (Figure 4).

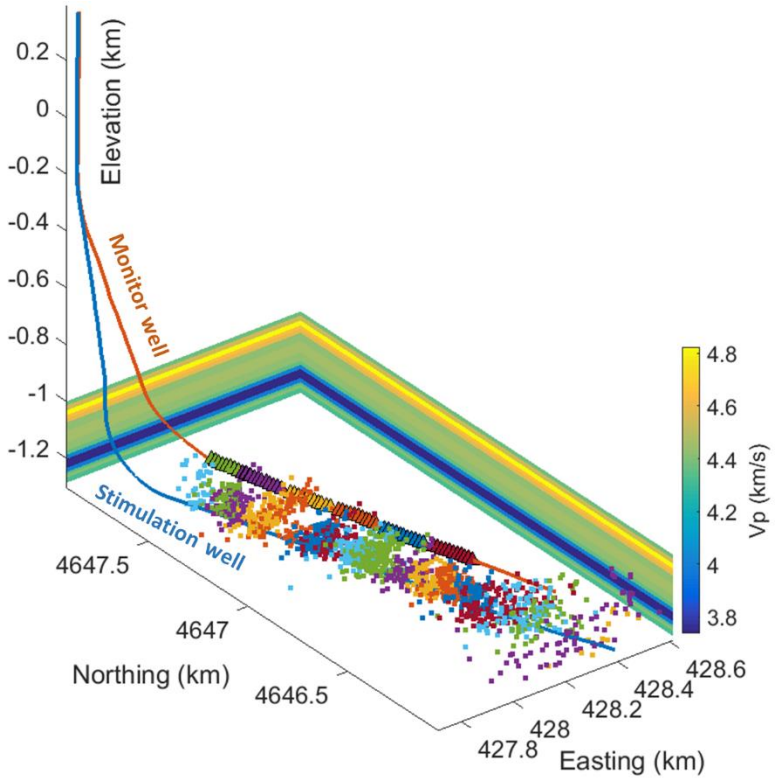

Figure 3: An array of eleven geophones (triangles) were moved on the monitoring well (orange) based on the location of eithteen stimulation stages. The microseismic event location (dots) around stimulation well (light blue) were processed by contractor. The geophone array is colored according to their various locations. Microseismic events are colored according to their associated stimulation stages.

Microseismic survey was conducted with an array of eleven three-component geophones. The geophone spacing in the array is around 15 m. The array was moved according to the location of hydraulic fracturing stages to minimize the noise due to source receiver distance.

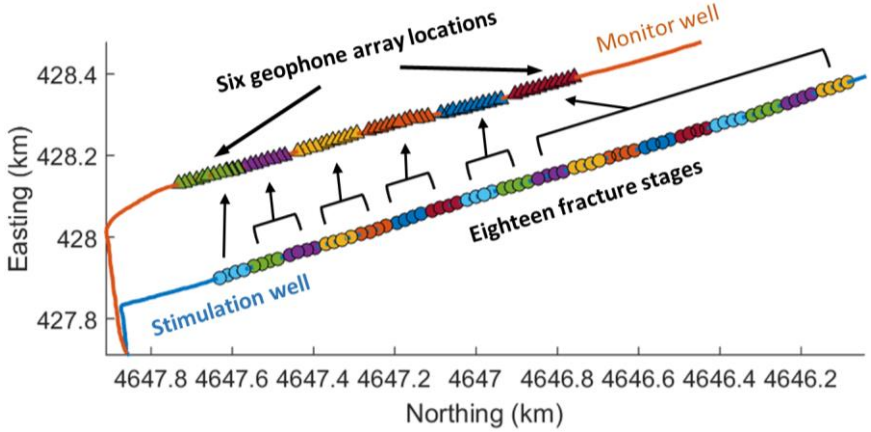

Figure 4: The stimulation was performed in 18 stages and the microseimsic signal was recorded by an array of 11 geophoens in the nearby monitoring well. The geophoen array was moved according to the stimuation stage location to reduce the error due to large observaton distance.

The microseismic waveform was processed by contractor and a total of 1842 events was detected and processed. The events number and geophones locations for each stimulation stage are shown in Table 1. In addition to these microseismic events, most of the perforation shots were recorded by the geophone array and can be used for velocity model calibration and location uncertainty analysis.

Table 1 Number of microseismic events in each stages and the associated geophone array locations.

Stage number	Events number	Array location	Stage number	Events number	Array location
1	11	1	10	224	2
2	66		11	168	
3	63		12	94	3
4	93		13	141	
5	130		14	101	4
6	106		15	120	
7	141		16	80	5
8	120		17	70	
9	80		18	34	6

Microseismic events were located by contractor. The velocity model used by contractor is an isotropic layered model built based on sonic log in the stimulation well as shown in Figure 3. The contractor estimated location of microseismic events are shown on Figure 3.

Observation of Head Wave

Head wave is commonly observed in waveforms of both perforation shots and microseismic events, especially those in the early fracking stages given their relatively large distance from the monitoring geophone array. We can begin by looking into the waveforms associated with two perforation shots shown in Figure 5.

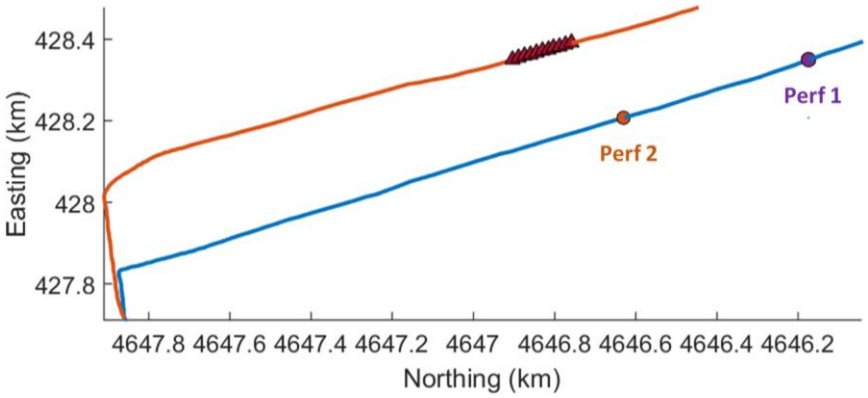

Figure 5: The location of two perforation shots whose waveform are shown by Figure 6 and Figure 7. The waveforms of Perf 1 and Perf 2 are shown in Figure 6 and Figure 7.

Figure 6 and Figure 7 show the waveforms recorded by the geophone array for Perf 1 and Perf 2 in Figure 5. The travel time of various phases for these two perforation shots are indicated by Figure 2. Figure 6 is a typical set of waveforms and moveout recorded by the geophone array. We can easily identify the head wave arrival based on its low amplitude and high velocity moveout. In this study, head wave, P and S wave arrival times are picked manually.

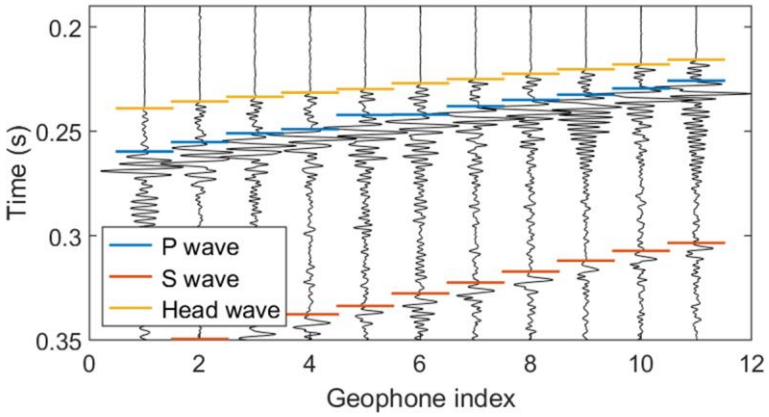

Figure 6: The waveform of Perf 1 recorded by the array of geophones. Head wave can be easily identified based on their low amplitude and high velocity moveout.

However, we cannot identify head wave arrival in Figure 7 since they arrive after and was buried by the stronger direct P-waves. This is due to their relatively short distance from the receivers.

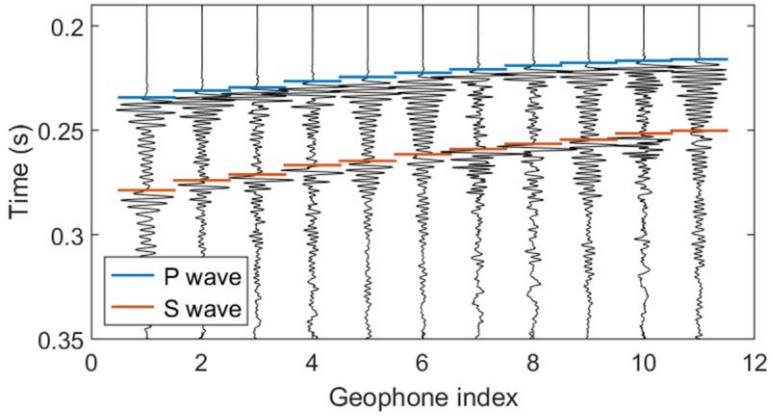

Figure 7: The waveform of Perf 2 recorded by the array of geophones. The Perf 2 is near the geophone array, thus, head wave arrives after the direct P arrival. We can not observe the head wave arrival in the waveform.

To further verify and analyze the head wave, the finite difference simulation of microseismic waveform propagation in the configuration of this project was conducted by Lawrence Livermore National Laboratory developed SW4 code. The configuration and velocity model was the same as that in Figure 1. The existence of head wave can be verified by the comparison between real and synthetic waveform as shown by Figure 8. Both the amplitude and arrival time of head wave in real data match the synthetic waveform pretty well.

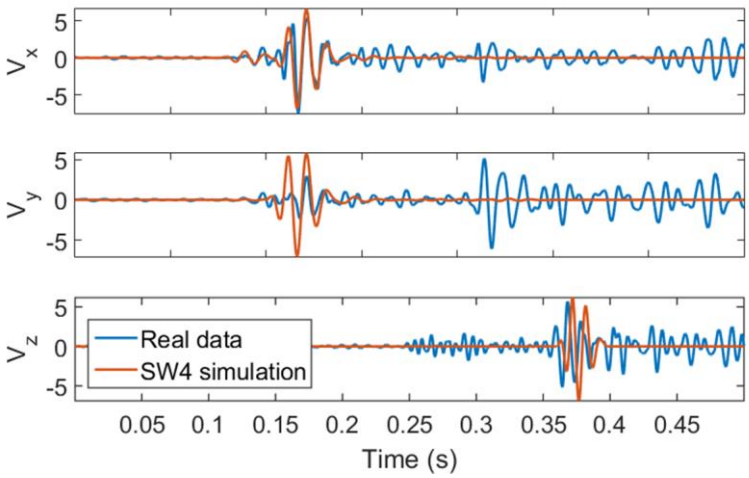

Figure 8: The synthetic waveform match the real data pretty well. This verified the existence of head wave. The difference on S-wave in the first two components might be because of the unknown source mechanism of the real event for simulation or the isotropic assumption in the velocity model.

Results and Discussion

Velocity model calibration

Since the original velocity model used by the contractor was a model built based on sonic logs, it is limited to the depth where the wells are situated. However, analysis on this velocity model shows that head wave will not take over direct arrival to be the first arrival as observed in the waveform. So the velocity model will need to be calibrated to waveform of perforation shots. This can be carried out by our developed Bayesian inversion code for microseismic event location. We can simply regard the velocity model as the model parameter **m** to be estimated and treat perforation shot location and the associate arrival time as the observable data **d**. From the velocity model calibration, we found the stimulation zone can be precisely characterized by the original velocity model ($V_p = 4.31\ km/s$ and $V_s = 2.67\ km/s$). However, the calibration also reveals the existence of a high velocity ($V_p = 6.01\ km/s$) zone approximately 70 m below the geophone array but there was no velocity information in the original model due to lack of sonic log.

Perforation shot location

We may locate the perforation shots whose locations are known to quantify the estimation accuracy. Our location result of perforation shots on stage two is shown by Figure 9 along with their true location. Please note that before the location of the perforation shots in this analysis, the velocity model was calibrated with all available perforation shots on stages other than stage two. Since the velocity model was not calibrated with perforation shots to be located, these perforation shots on stage two can treated as normal microseismic events and used for location uncertainty analysis.

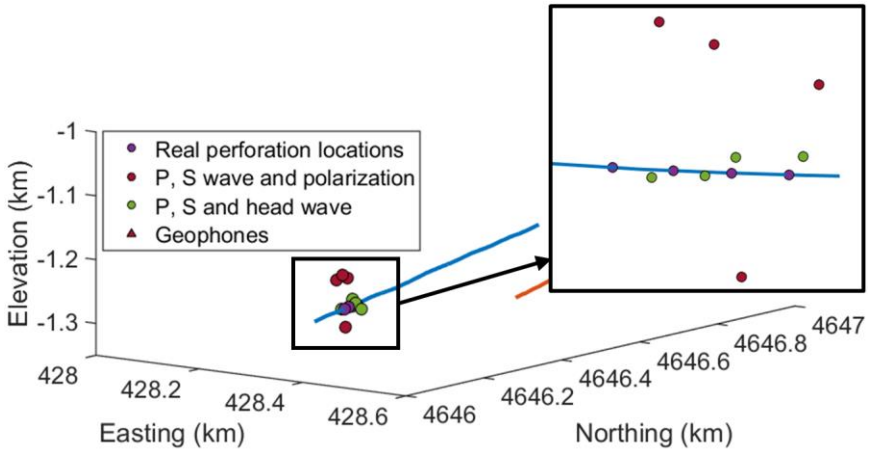

Figure 9: Comparison on estimated perforation shots location and the true perforation location. The perforation shot location estimated with P, S and head wave arrivals is more accurate comparing to the location estimated with traditional P, S arrivals and polarization method.

What is also displayed in Figure 9 is the location result with the traditional method, which use P, S-wave arrivals and direct P-wave polarization. The polarization of direct P-wave is calculated by a hodograms eigenvector method. From the comparison between these results, we found the method using head wave gives an average error of $15\ m$ while the traditional method with polarization gives an error of $49\ m$. This demonstrates the effectiveness and accuracy of our proposed location method with head wave arrivals.

Relocation of microseismic events on stage two

The map view of the microseismic event location provided by the contractor is shown in Figure 10. Apparently, the microseismic event location on stages two is significantly more scattered than those on later stages. One possible explanation of the scattering is because of the larger stimulated reservoir volume for stage two. Another explanation is simply because of the large location uncertainty due to the long distance of stage two from the geophone array.

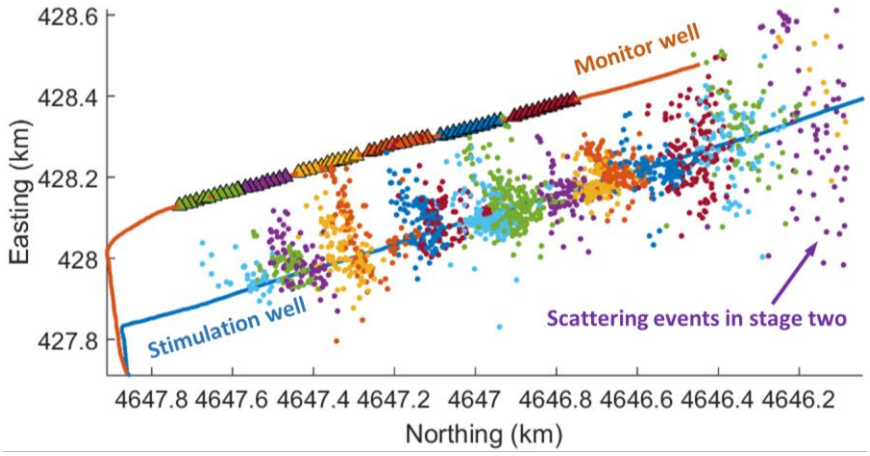

Figure 10: Map view of microseismic event location processed by contractor. The event location on stage two is more scattering than later stages.

To answer this question, we relocated microseismic events on stage two with head wave arrival times instead of direct P-wave polarizations. In the original event catalog, there were 66 events on stage two. We were able to confidently pick head wave for 31 events among them. The result is shown in Figure 11. Apparently, the relocated events are much less scattering than the result provided by contractor. This shows that the scattering of stage two events in the original catalog was due to the large uncertainty in the estimation. Also, it exhibits the effectiveness of accounting for head wave in microseismic event location to improve location accuracy.

The large amount of head wave enable us to make effective use of them to reduce location uncertainty due to large source receiver distance and large uncertainty in P-wave polarization. This method is especially useful for situations where geophone cannot be put to adjacent of stimulation zone due to physical limitations. Whenever available, the head wave can be used to reduce uncertainty with location. Since location estimation with head wave was usually more accurate, it may be possible to improve nearby events location estimation with these accurate event location by means of double-difference (Waldhauser and Ellsworth, 2000) or matched field processing (Baggeroer and Kuperman, 1993; Harris and Kvaerna, 2010).

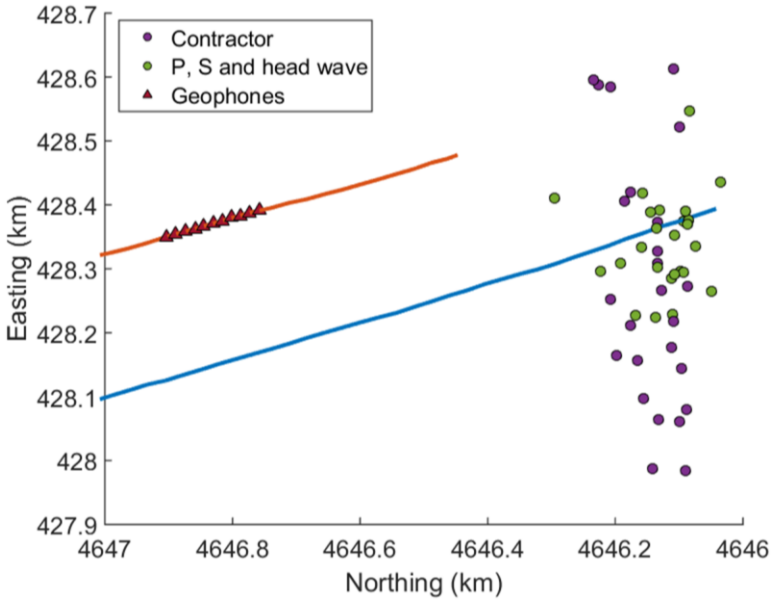

Figure 11: The microseismic event location estimated with P, S and head wave arrival is less scattering comparing with the microseismic event location processed by the contractor.

Since it is hard to pick head wave arrives after direct P-wave arrival, we will be forced to use polarization to constrain the event direction for stages near the geophone. This traditional polarization method is problematic as we have shown. So the traditional acquisition practice will need to be improved. We would propose a two array acquisition geophone for single horizontal well hydraulic fracturing monitoring. One array should be as near to the stimulation zone as possible. And the other array should be at relatively large distance from the stimulation zone for head wave monitoring. This acquisition geometry will be able to use multiple arrivals as well as obtain high S/N ratio.

Conclusion

The existence of head wave in microseismic survey in Marcellus shale is observed and verified. A Bayesian inverse framework was developed for microseismic event location. The location result of perforation shots using the developed method verified that the accounting for head wave arrival time as a substitution of P-wave polarization indeed improves the microseismic location accuracy. The analysis of relocation result on microseismic events on stage two shows that the scattering of stage two events in original catalog is a result of large uncertainty associated with the original location method. This scattering can be reduced by our proposed method. Based on the result, we proposed a two array acquisition geometry for single horizontal well hydraulic fracturing. This will enable us to improve microseismic event location accuracy.

References

Baggeroer, Arthur B., and William A. Kuperman. "Matched field processing in ocean acoustics." In Acoustic Signal Processing for Ocean Exploration, pp. 79-114. Springer Netherlands, 1993.

Cipolla, Craig, S. Maxwell, M. Mack, and Robert Downie. "A practical guide to interpreting microseismic measurements." In SPE/EAGE European Unconventional Resources Conference & Exhibition-From Potential to Production. 2012.

Dong, Wenjie, and M. Nafi Toksöz. "Borehole seismic-source radiation in layered isotropic and anisotropic media: Real data analysis." Geophysics 60, no. 3 (1995): 748-757.

Douglas, Alan. "Joint epicentre determination." Nature 215 (1967): 47-48.

Dreger, Douglas, Robert Uhrhammer, Michael Pasyanos, Joseph Franck, and Barbara Romanowicz. "Regional and far-regional earthquake locations and source parameters using sparse broadband networks: A test on the Ridgecrest sequence." Bulletin of the Seismological Society of America 88, no. 6 (1998): 1353-1362.

Drew, Julian Edmund, H. David Leslie, Philip Neville Armstrong, and Gwenola Michard. "Automated microseismic event detection and location by continuous spatial mapping." In SPE Annual Technical Conference and Exhibition. Society of Petroleum Engineers, 2005.

Duncan, P. and Eisner, L.. "Reservoir characterization using surface microseismic monitoring." Geophysics 75, no. 5 (2010): 75A139-75A146.

Eisner, Leo and Le Calvez, Joel Herve. "New Analytical Techniques To Help Improve Our Understanding of Hydraulically Induced Microseismicity and Fracture Propagation." (2007).

Eisner, Leo, Peter M. Duncan, Werner M. Heigl, and William R. Keller. "Uncertainties in passive seismic monitoring." The Leading Edge 28, no. 6 (2009): 648-655.

Gaiser, James E., Terrance J. Fulp, Steve G. Petermann, and Gary M. Karner. "Vertical seismic profile sonde coupling." Geophysics 53, no. 2 (1988): 206-214.

Harris, David B., and Tormod Kvaerna. "Superresolution with seismic arrays using empirical matched field processing." Geophysical Journal International 182, no. 3 (2010): 1455-1477.

Hayles, Kristin, Robert L. Horine, Steve Checkles, and J. P. Blangy. "Comparison of microseismic results from the Bakken Formation processed by three different companies: Integration with surface seismic and pumping data: 81st Annual International Meeting." In SEG, Expanded Abstracts, vol. 1468. 2011.

Li, Junlun, Chang Li, Scott A. Morton, Ted Dohmen, Keith Katahara, and M. Nafi Toksöz. "Microseismic joint location and anisotropic velocity inversion for hydraulic fracturing in a tight Bakken reservoir." Geophysics 79, no. 5 (2014): C111-C122.

Maxwell, Shawn. Microseismic imaging of hydraulic fracturing: Improved engineering of unconventional shale reservoirs. No. 17. SEG Books, 2014.

Maxwell, S. C., J. Rutledge, R. Jones, and M. Fehler. "Petroleum reservoir characterization using downhole microseismic monitoring." Geophysics 75, no. 5 (2010): 75A129-75A137.

Maxwell, Shawn. "Microseismic location uncertainty." CSEG Recorder, April (2009).

Maxwell, Shawn. "Microseismic: Growth born from success." The Leading Edge 29, no. 3 (2010): 338-343.

Myers, Stephen C., Gardar Johannesson, and William Hanley. "A Bayesian hierarchical method for multiple-event seismic location." Geophysical Journal International 171, no. 3 (2007): 1049-1063.

Myers, Stephen C., Gardar Johannesson, and William Hanley. "Incorporation of probabilistic seismic phase labels into a Bayesian multiple-event seismic locator." Geophysical Journal International 177, no. 1 (2009): 193-204.

Oliver, Dean S., Albert C. Reynolds, and Ning Liu. Inverse theory for petroleum reservoir characterization and history matching. Cambridge University Press, 2008.

Parra, J. O., C. L. Hackert, P-C. Xu, and Hughbert A. Collier. "Attenuation analysis of acoustic waveforms in a borehole intercepted by a sand-shale sequence reservoir." The Leading Edge 25, no. 2 (2006): 186-193.

Parra, Jorge O., Chris L. Hackert, Anthony W. Gorody, and Valeri Korneev. "Detection of guided waves between gas wells for reservoir characterization." Geophysics 67, no. 1 (2002): 38-49.

Poliannikov, Oleg V., Michael Prange, Alison E. Malcolm, and Hugues Djikpesse. "Joint location of microseismic events in the presence of velocity uncertainty." Geophysics 79, no. 6 (2014): KS51-KS60.

Tarantola, Albert, and Bernard Valette. "Inverse problems= quest for information." J. geophys 50, no. 3 (1982): 150-170.

Tarantola, Albert. Inverse problem theory and methods for model parameter estimation. siam, 2005.

Waldhauser, Felix, and William L. Ellsworth. "A double-difference earthquake location algorithm: Method and application to the northern Hayward fault, California." Bulletin of the Seismological Society of America 90, no. 6 (2000): 1353-1368.

Warpinski, Norm. "Microseismic monitoring: Inside and out." Journal of Petroleum Technology 61, no. 11 (2009): 80-85.

Zhang, Zhishuai, Behnam Jafarpour, and Lianlin Li. "Inference of permeability heterogeneity from joint inversion of transient flow and temperature data." Water Resources Research 50, no. 6 (2014): 4710-4725.

Zimmer, Ulrich. "Localization of microseismic events using headwaves and direct waves." In 2010 SEG Annual Meeting. Society of Exploration Geophysicists, 2010.

Zimmer, Ulrich. "Microseismic design studies." Geophysics 76, no. 6 (2011): WC17-WC25.